Separation Science and Technology
Publication details, including instructions for authors and subscription information:
http://www.informaworld.com/smpp/title~content=t713708471

Sensitivity Analysis of Air Gap Membrane Distillation

Fahmi A. Abu Al-Rub[a]; Fawzi Banat[b]; Khalid Bani-Melhem[c]
[a] Chemical and Petroleum Engineering Department, United Arab Emirates University, Al-Ain, United Arab Emirates [b] Department of Chemical Engineering, Jordan University of Science and Technology, Irbid, Jordan [c] Department of Building, Civil and Environmental Engineering, Concordia University, Montreal, Canada

Online publication date: 09 August 2003

To cite this Article Al-Rub, Fahmi A. Abu , Banat, Fawzi and Bani-Melhem, Khalid(2003) 'Sensitivity Analysis of Air Gap Membrane Distillation', Separation Science and Technology, 38: 15, 3645 — 3667
To link to this Article: DOI: 10.1081/SS-120024222
URL: http://dx.doi.org/10.1081/SS-120024222

SEPARATION SCIENCE AND TECHNOLOGY
Vol. 38, No. 15, pp. 3645–3667, 2003

Sensitivity Analysis of Air Gap Membrane Distillation

Fahmi A. Abu Al-Rub,[1,*] Fawzi Banat,[2] and Khalid Bani-Melhem[3]

[1]Chemical and Petroleum Engineering Department, United Arab Emirates University, Al-Ain, United Arab Emirates
[2]Department of Chemical Engineering, Jordan University of Science and Technology, Irbid, Jordan
[3]Department of Building, Civil and Environmental Engineering, Concordia University, Montreal, Quebec, Canada

ABSTRACT

In this study, parametric sensitivity analysis using dimesionless sensitivity analysis and temperature polarization was used to investigate the sensitivity of the mass flux to the different parameters associated with the air gap membrane distillation (AGMD) process for pure water production. The model of AGMD used in this study is the approximate model proposed by Jonsson et al., which neglects the temperature polarization effect. The effect of temperature polarization is studied

*Correspondence: Fahmi A. Abu Al-Rub, Chemical and Petroleum Engineering Department, United Arab Emirates University, P.O. Box 17555, Al-Ain, United Arab Emirates; Fax: +971-3-762-4262; E-mail: f.rub@uaeu.ac.ae.

DOI: 10.1081/SS-120024222
0149-6395 (Print); 1520-5754 (Online)

www.dekker.com

MARCEL DEKKER, INC.
270 Madison Avenue, New York, New York 10016

using another model developed by Banat and Simandl. The results obtained show that the mass flux of pure water production is highly sensitive to the feed bulk temperature, membrane porisity at low porosity values, and air gap width. Results also show that increasing the membrane thickness decreases the mass flux of pure water and decreases the temperature polarization effect. In addition, results show that the temperature polarization effect becomes significant as feed bulk temperature increases. Increasing the film heat-transfer coefficients, increasing the diffusion path, or decreasing the membrane porosity can reduce the temperature polarization effect significantly.

Key Words: Membrane distillation; Sensitivity; Air gap; Flux.

INTRODUCTION

Membrane distillation (MD) is a thermally driven separation process where solutions with different temperatures are separated by a microprous hydrophobic membrane that acts as a physical support. The vapor pressure gradient resulting from the temperature difference across the membrane serves as the driving force for the transfer of the components from the warm feed side to the cold permeate side.[1–6] In direct contact membrane distillation (DCMD), the liquid phases are in direct contact with both sides of membrane, while the gaseous phase is trapped within the membrane pores.[1,6] Air gap membrane distillation (AGMD) is similar to DCMD, however, an additional diffusion path is added to the membrane thickness, so a coolant plate is used on the permeate side while the feed is subjected to the membrane surface. The evaportaion components are condensed on the other surface of the coolant plate, as shown in Figure 1. The advantages of this system are that it reduces heat loss by conduction through the membrane and that wetting of some pores of membrane does not spoil the permeate quality. On the other hand, AGMD has the disadvantage that air gap width gives rise to higher heat- and mass-transfer resistances.

The process may be attractive for ultrapure water production, for desalination of brackish or sea waters, or for the concentration of dilute aqueous solutions. Potential applications of AGMD have been discussed by many researchers and some experimental and theoretical studies have also been described.[7–17] AGMD was first proposed by Jonsson et al.[8] They illustrated theoretically the effects of different parameters involved in the air gap membrane distillation system on the mass flux. Temperature polarization effect was neglected in their model. Kimura et al.[10] studied experimentally the technique of AGMD for a variety of aqueous solutions with different

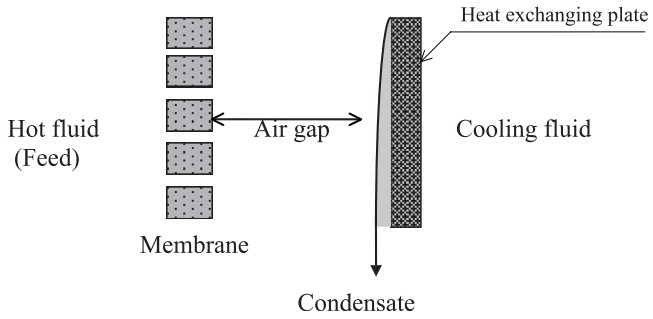

Figure 1. Air gap membrane distillation.

viscosity values using flat sheets of polytetrafluoroethlene (PTFE). They concluded that the permeate flux is dependent on viscosity. Kubota et al.[11] carried out experiments for seawater desalination. They investigated the effect of process parameters on heat efficiency. They found that heat loss in the tested modules was large. Ohta et al.[12,13] investigated experimentally the effect of membrane material on the thermal efficiency of the process of desalination of water. Udriot et al.[14] studied experimentally the separation of aqueous mixtures involving azeotropic points. HCl–water and propionic acid–water were the studied systems. Banat et al.[15] studied theoretically the effect of inert gases in breaking the formic acid–water azeotropic point by the AGMD and found that heavy inert gases, such as sulfure hexafluoride, help more in breaking the azeotropic point than lighter gases, such as air and helium. Liu et al.[16] studied theoretically and experimentally the use of AGMD in the extraction of pure water from different aqueous solutions. Zhu et al.[17] investigated the application of an ultrasonic irradiation technique to AGMD system to enhance the permeability of the membrane distillation of various aqueous solutions. Kurokawa et al.[18] studied the effect of concentration polarization using concentrated solutions of Li, Br, and H_2SO_4, using PTFE membranes. They attributed the reduction in flux when feed concentration was increased to concentration and temperature polarization. Banat and Simandl[7] developed a mathematical model for an AGMD module used for desalination. The developed mathematical model was verified with a wide range of experimental data. However, to the authors knowledge, all of the work on AGMD did not study the relative effect of the associated parameters on the mass flux.

The objective of this study was to develop a relatively simple criterion to determine the sensitivity of the flux to the input parameters associated in

Marcel Dekker, Inc.
270 Madison Avenue, New York, New York 10016

the mathematical model. Parametric sensitivity analysis was applied to the model proposed by Jonnson et al.,[8] The advantage of this model over the other models mentioned in the literature is the explicit dependence of the permeate flux on the different input parameters involved. On the other hand, the main disadvantage of the model is that it neglects the temperature polarization effect. To analyze the significance of this assumption, a general model of AGMD, proposed by Banat and Simandl,[7] was used. The analysis was applied to the case of pure water production, which simulates the desalination application.

THEORY

Heat- and Mass-Transfer Analysis of AGMD

Jonsson et al.[8] proposed an approximate model of evaporation through microporous membranes. They neglected the influence of the heat and mass transfer from the bulk of the hot solution to the membrane surface and the heat transfer through the condensed film. The dependence of diffusivity on temperature and concentration was taken into consideration using the equation:

$$cD = 6.3*10^{-5}\sqrt{T} \tag{1}$$

Eq. (1) is based on experimental diffusion in water vapor–air mixtures at temperatures around 40°C.[19] Further, they assumed that diffusion through noncondensable air is the mechanism of transport. Convection in the pores and air gap is neglected. This assumption is justified by the fact that the space in the air gap consists of a relatively dense net. The final form of the proposed model was given by[8]

$$N = 6.3*10^{-5}\frac{M}{\left[\dfrac{b}{\varepsilon\sqrt{T_h}}+\dfrac{w}{\sqrt{T_c}}\right]}\cdot\ln\frac{P-P_c}{P-P_h} \tag{2}$$

where b is the membrane thickness, ε is the porosity of the membrane, w is the air gap width, T_h and T_c are the hot and cold temperatures respectively, and M is the molecular weight of water. As evidenced from Eq. (2), temperature polarization was not taken into account in this equation. Temperature polarization occurs in a membrane distillation operation as a result of temperature gradient across the membrane. This phenomenon can be analyzed using the temperature polarization factor (TPF), θ, which is defined as the temperature difference between the evaporation surface and

Marcel Dekker, Inc.
270 Madison Avenue, New York, New York 10016

the condensation surface divided by the temperatrure difference between the bulk streams, thus

$$\theta \equiv \frac{T_m - T_p}{T_h - T_c} \tag{3}$$

where T_m is the temperture of the membrane side at which the evaporation takes place and T_p is the temperature of the plate surface at which the condensation takes place. Numerically, TPF shows the percentage deviation of the interfacial temperatures T_m and T_p from the bulk temperatures T_h, T_c, respectivly. Thus, when $\theta \rightarrow 0.0$, the interfacial temperatures approach each others. While as $\theta \rightarrow 1$, the difference between the interfacial temperatures $(T_m - T_p)$ will approach the difference between the bulk temperatures $(T_h - T_c)$ and, hence, the polarization effect is not significant.

The effect of temperature polarization was studied using the model developed by Banat and Simandl.[7] The general form of Banat and Simandl model is given by[7]

$$N = \frac{\varepsilon PDM}{RT_{av}(b\tau + w)P^*_{c,lm}}(P^*_m - P^*_p) \tag{4}$$

where ε is membrane porosity, b is the membrane thickness, τ is the tortuosity, M is the molecular weight of water, D is the diffusion coefficient, P* is the partial pressure of water vapor, and $P^*_{c,lm}$ is the log mean partial pressure difference of the stagnant compound defined as:

$$P^*_{c,lm} = \frac{P^*_{c,m} - P^*_{c,p}}{\ln \dfrac{P^*_{c,m}}{P^*_{c,p}}} \tag{5}$$

The subscript m and p are assigned for the membrane side and permeate side, respectively. Calculating the TPF from the Banat model requires the knowledge of the interfacial temperatures T_m and T_p, which are given by the following equations[7]

$$T_m = T_h - \frac{U_T}{h_h}\left((T_h - T_c) + \frac{N\lambda}{h^*}\right) \tag{6}$$

$$T_p = T_c + \frac{U_T}{h_c}\left((T_h - T_c) + \frac{N\lambda}{h^*}\right) \tag{7}$$

where h_h is the total warm region heat-transfer coefficient, h_c is the total cold region heat-transfer coefficient, h* is the heat-transfer coefficient in the gaseous phase corrected for the effect of finite mass transfer, and U_T is

MARCEL DEKKER, INC.
270 Madison Avenue, New York, New York 10016

the overall heat-transfer coefficient involving h_h, h_c, and h*. The details of the derivation of Eqs. (6) and (7) can be found elsewhere.[7]

Sensitivity Analysis

The method of dimensionless normalized sensitivity factors[1,20] was used to study the sensitivity of all parameters involved in Jonsson et al. model. Before proceeding, the following sensitivity factors are defined.

1. The first-order sensitivity factor of any model response R with respect to any of the model input parameters P_i is defined as[21]

$$s(R, P_i) \equiv \frac{\partial R}{\partial P_i} \tag{8}$$

2. The normalized dimensionless sensitivity factor is defined as[1,20,21]

$$S(R, P_i) \equiv \frac{\partial \ln R}{\partial \ln P_i} = \frac{Pi}{R}\frac{\partial R}{\partial P_i} = s(R, P_i)\frac{P_i}{R} \tag{9}$$

where P_i is any parameter that may affect R. In the case of pure water, R represents the mass flux (N) and P_i may be any one of the input parameters affecting N, i.e., T_h, T_c, w, b, or ε. As the studied parameters are not dimensionally homogeneous, normalized sensitivity factors provide more significance about the physical meaning because they are dimensionless factors.

According to the above definitions, expressions for normalized sensitivity factors can be found using Eqs. (2), (8), and (9)

$$S(N, w) = \frac{-w}{\sqrt{T_c}\left[\dfrac{b}{\varepsilon\sqrt{T_h}} + \dfrac{w}{\sqrt{T_c}}\right]} \tag{10}$$

$$S(N, b) = \frac{-b}{\varepsilon\sqrt{T_h}\left[\dfrac{b}{\varepsilon\sqrt{T_h}} + \dfrac{w}{\sqrt{T_c}}\right]} \tag{11}$$

$$S(N, \varepsilon) = \frac{+b}{\varepsilon\sqrt{T_h}\left[\dfrac{b}{\varepsilon\sqrt{T_h}} + \dfrac{w}{\sqrt{T_c}}\right]} \tag{12}$$

Marcel Dekker, Inc.
270 Madison Avenue, New York, New York 10016

$$S(N, T_h) = \frac{+0.5b}{\varepsilon\sqrt{T_h}\left[\frac{b}{\varepsilon\sqrt{T_h}} + \frac{w}{\sqrt{T_c}}\right]} + \frac{\lambda M P_h}{RT_h(P - P_h)\ln\left(\frac{P - P_c}{P - P_h}\right)} \quad (13)$$

$$S(N, T_c) = \frac{0.5w}{\sqrt{T_c}\left[\frac{b}{\varepsilon\sqrt{T_h}} + \frac{w}{\sqrt{T_c}}\right]} - \frac{\lambda M P_c}{RT_c(P - P_c)\ln\left(\frac{P - P_c}{P - P_h}\right)} \quad (14)$$

RESULTS AND DISCUSSION

Effect of the Operating Conditions

Effect of the Feed Bulk Temperature

Figure 2 shows the effect of the variation of the feed bulk temperature, at constant coolant temperature, on the mass flux. Figure 2 shows that the

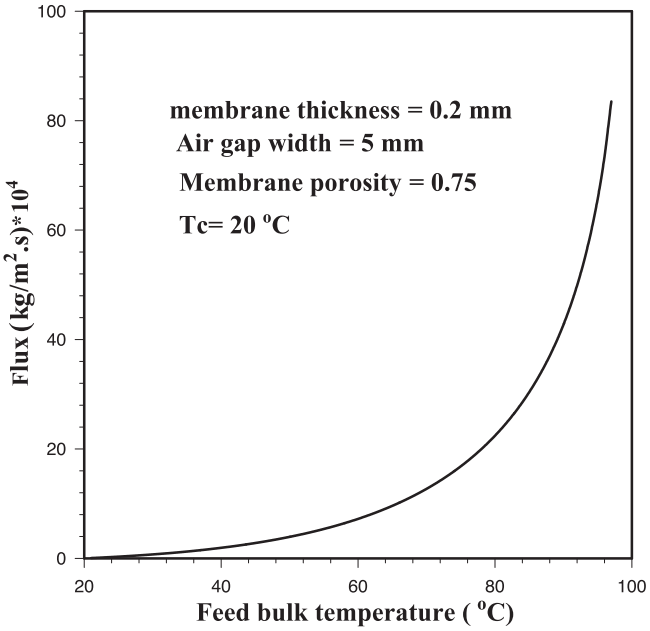

Figure 2. Effect of feed bulk temperature on mass flux.

MARCEL DEKKER, INC.
270 Madison Avenue, New York, New York 10016

mass flux increases exponentially by increasing the feed bulk temperature. This is due to the typical relationship between vapor pressure and temperature, which is presented by Antoine's equation. Increasing the feed bulk temperature increases the vapor pressure of water and, hence, the driving force across the membrane increases. A similar trend was obtained experimentally by Liu et al.[16] using different aqueous solutions.

The response of normalized mass flux sensitivity to the feed bulk temperature, at constant coolant temperature, is shown in Figure 3. The normalized sensitivity factor of feed bulk temperature from the Jonsson et al. model consists of two terms, as shown in Eq. (13). Obviously, the first term of Eq. (13) is negligible in comparison with the second term, as shown in Figure 4.

Figure 3 shows that the normalized sensitivity factor $S(N,T_h)$ is always greater than 1, which means that the percentage change in the transmembrane flux, due to a given change in the feed bulk temperature only, is always greater than the percentage that is considered for T_h.

The normalized sensitivity of the mass flux to the feed bulk temperature, shown in Figure 3, shows a sharp maximum at lower temperatures of T_h and starts to decrease by increasing the temperature to a point at which the

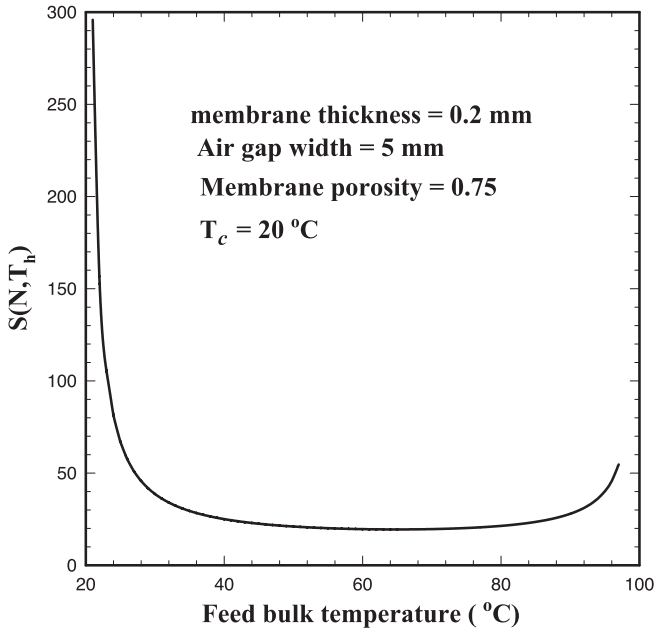

Figure 3. Response of $S(N,T_h)$ to feed bulk temperature.

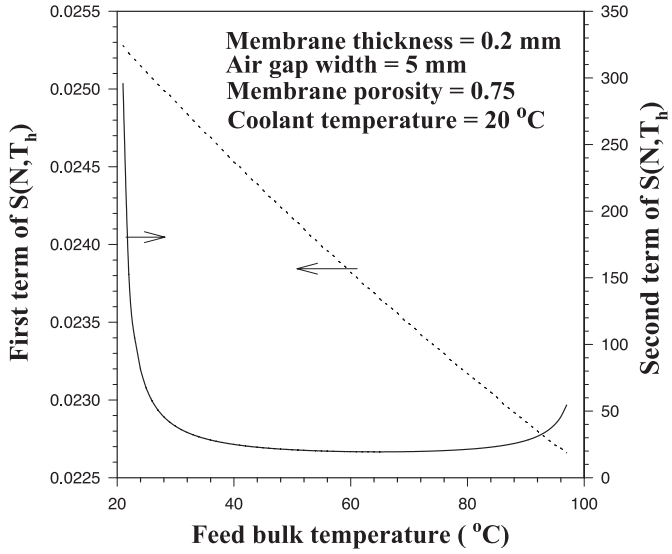

Figure 4. Response of first term and second term of $S(N,T_h)$ in Eq. (13) to feed bulk temperature.

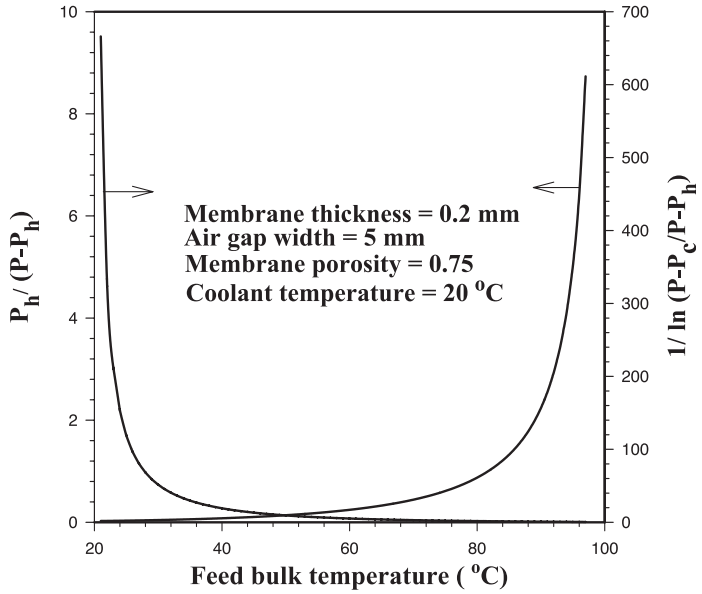

Figure 5. Response of $(P_h/P - P_h)$ and $1/\ln(P - P_c/P - P_h)$ to feed bulk temperature.

MARCEL DEKKER, INC.
270 Madison Avenue, New York, New York 10016

sensitivity again increases. The behavior of the dependence of $S(N,T_h)$ on T_h suggests that the figure can be divided into three regions.

Region 1: in this region, the sensitivity of the mass flux to the feed temperature decreases very sharply with increasing the feed bulk temperature. This behavior is expected to be at lower feed bulk temperature. In this region, $(T_h \rightarrow T_c)$, hence, $(P_h \rightarrow P_c)$ then $\left(\frac{P-P_c}{P-P_h}\right) \rightarrow 1$ or $\left(\ln\frac{P-P_c}{P-P_h}\right) \rightarrow 0.0$, which reflects the higher numerical values of $S(N, T_h)$ at lower feed temperatures, as illustrated in Figure 5. Generally speaking, it can be said that in this region, the sensitivity of mass flux to the driving force across the membrane overcomes the sensitivity of mass flux to feed bulk temperature, which is obtained from the sensitivity of vapor pressure at high temperatures. In this region, the effect of the term $\left(\ln\frac{P-P_c}{P-P_h}\right)$ in Eq. (13) dominates over the effect of the term $\left(\frac{P_h}{P-P_h}\right)$ in $S(N,T_h)$, as shown in Figure 5.

Region 2: in this region, the effect of the term $\left(\ln\frac{P-P_c}{P-P_h}\right)$ in Eq. (13) starts to decrease and the effect of the vapor pressure in the term $\left(\frac{P_h}{P-P_h}\right)$, resulting from the increase in T_h, starts to increase. Thus, the net result is a constant normalized sensitivity in this region.

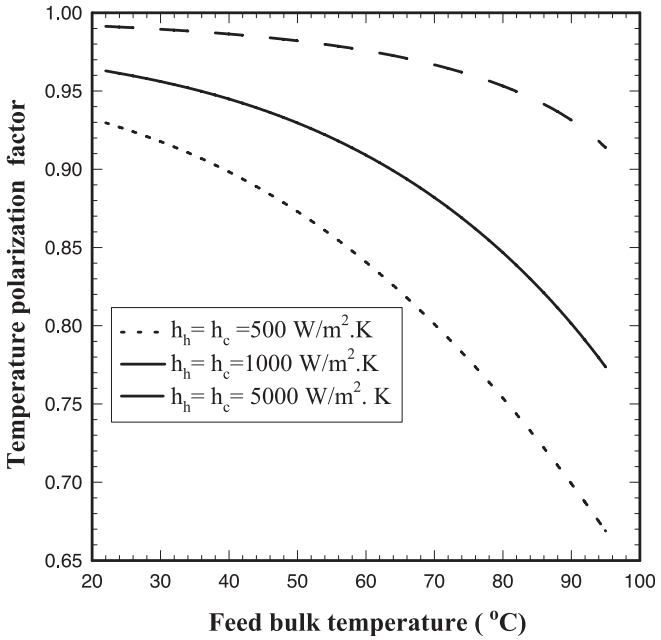

Figure 6. Effect of feed bulk temperature on temperature polarization factor.

Marcel Dekker, Inc.
270 Madison Avenue, New York, New York 10016

Region 3: in this region; the sensitivity of the mass flux to the feed bulk temperature appears as a result of effect of the increase in temperature on vapor pressure. In this region, the effect of the term $\left(\frac{P_h}{P-P_h}\right)$ dominates over the term $\left(\ln\frac{P-P_c}{P-P_h}\right)$, as shown in Figure 5.

Figure 6 shows the effect of feed bulk temperature on TPF, as defined in Eq. (3). The Banat and Simandl model was solved for three different values of heat-transfer coefficients, 500, 1000, and 5000 $W/m^2 \cdot K$. The polarization factor decreases by increasing the feed bulk temperature. An increase in feed bulk temperature increases the difference between T_h and T_c and also the difference between T_m and T_p. The increase in the difference $(T_m - T_p)$ will be small in comparison with the increase in difference $(T_h - T_c)$, thus, the net result is a decrease in temperature polarization factor as is shown from Eq. (5). On the other hand, increasing

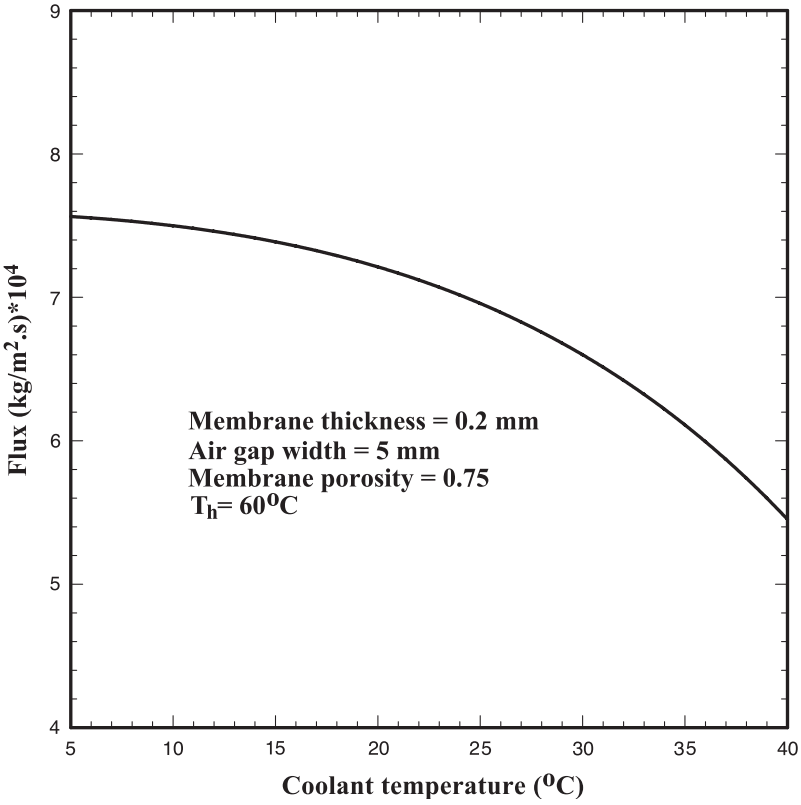

Figure 7. Effect of coolant temperature on mass flux.

the heat-transfer coefficients increases the mass flux. This occurs because increasing the heat-transfer coefficients decreases the temperature polarization, so the interfacial temperatures will approach the bulk temperatures. Thus, TPF approaches unity.

Obviously, one can conclude that the temperature polarization effect can be neglected only at lower feed bulk temperature if the operation is at lower heat-transfer coefficients. Similarly as h_h and h_c become very large (e.g., 10,000 $W/m^2 \cdot K$), the temperature polarization factor decreases slightly with feed bulk temperature and, thus, the effect of feed bulk temperature on TPF is nearly neglected. This makes the assumption of neglecting the polarization effect valid for the parameter T_h.

Effect of the Coolant Temperature

In Figure 7, the mass flux of pure water system is plotted as a function of the coolant temperature. Figure 7 shows that the mass flux decreases by increasing the coolant temperature. This is due to the decrease in the driving force between the bulk temperatures.

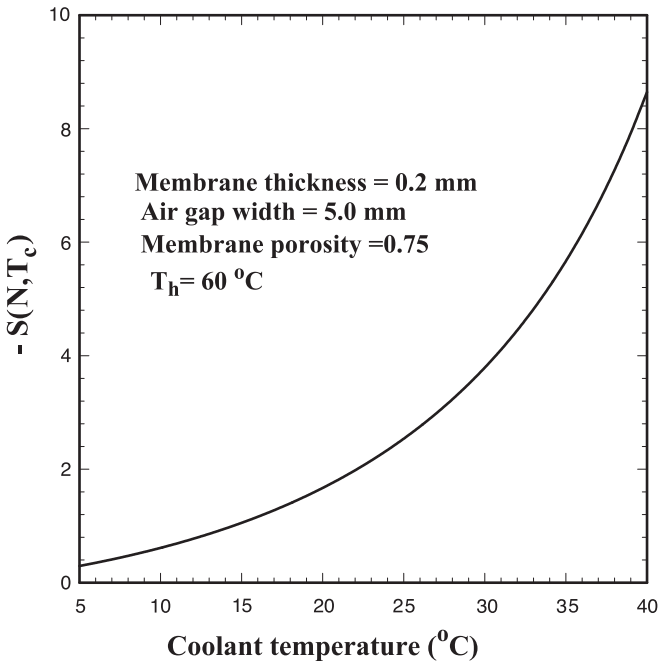

Figure 8. Response of $S(N,T_c)$ to coolant temperature.

Figure 8 shows the normalized sensitivity of mass flux to coolant temperature. As shown in Figure 8, $S(N,T_c)$ increases negatively with increasing T_c. The negative values of $S(N,T_c)$ are in agreement with the fact that the increase in T_c causes a decrease in the mass flux. At lower values of T_c, the driving force between T_h and T_c will be maximum and the normalized sensitivity factor approaches zero. As T_c increases, the sensitivity of the flux to T_c becomes more pronounced. This result is in agreement with that obtained in the first region, in Figure 3, when $T_h \rightarrow T_c$.

A direct comparison between Figures 5, 7, and 8, shows that the normalized sensitivity factor $S(N,T_c)$ can be considered only as a tool for measuring the sensitivity of mass flux to the driving force across the membrane. This is attributed to the lower sensitivity of vapor pressure at lower temperatures.

Figure 9 shows that the response of the first term in $S(N,T_c)$ in Eq. (14) is nearly negligible in comparison with the response of the second term, as it was obtained for $S(N,T_h)$.

The effect of coolant temperature on temperature polarization factor is shown in Figure 10 with the heat transfer coefficients as parameters. Apparently, the polarization factor decreases by increasing the coolant

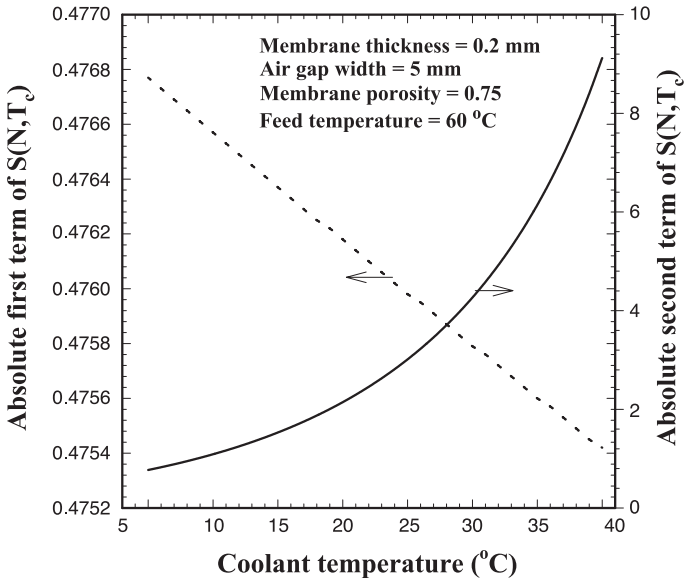

Figure 9. Response of first term and second term of $S(N,T_c)$ in Eq. (14) to coolant temperature.

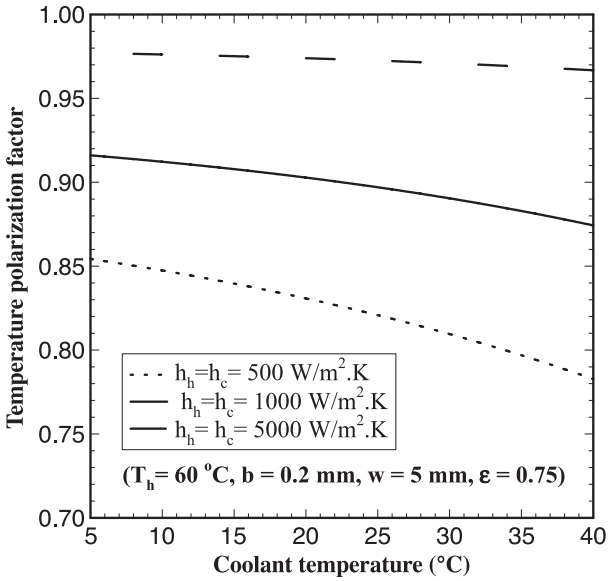

Figure 10. Effect of coolant temperature on polarization factor.

temperature, as is the case for T_h, this is because an increase in T_c decreases the overall temperature driving force, $(T_h - T_c)$, and also the temperature driving force across the membrane, $(T_m - T_p)$. Eventually, the difference between $(T_m - T_p)$ decreases more rapidly than the difference between $(T_h - T_c)$, hence, the net result is a decrease in TPF. On the other hand, the polarization effect is nearly negligible for very large heat-transfer coefficients (e.g., 10,000 $W/m^2 \cdot K$). This is due to the same reason previously discussed. These results show that no real and direct conclusion can be obtained from the polarization factor about the parametric sensitivity of flux toward either T_h or T_c, as it was obtained from normalized sensitivity factors.

Effect of Membrane Characteristics

In Eqs. (10) and (11), it can be shown that the normalized sensitivity factors of the air gap width and membrane thickness are dependent and related by the relation

$$S(N, b) + S(N, w) = -1 \tag{15}$$

and the normalized sensitivity factors of the membrane thickness and that for membrane porosity are related by the relation

$$S(N, \varepsilon) + S(N, b) = 0.0 \tag{16}$$

This means that the normalized sensitivity factors of the membrane characteristics are dependent and, thus, the normalized sensitivity factors can be determined if only one of them is calculated.

Effect of Membrane Porosity

The variation of mass flux with membrane porosity, predicted from the Jonsson et al. model, is shown in Figure 11. The figure shows that the mass flux increases with increases in the membrane porosity. This increase in the mass flux is attributed to the increase in the net area available for vapor diffusion across the membrane. However, the mass flux increases sharply at lower membrane porosity and it tends to increase slowly as the porosity increases beyond 40%.

Figure 12 shows the response of the normalized mass flux sensitivity to membrane porosity. At lower porosity, the mass flux will be very sensitive

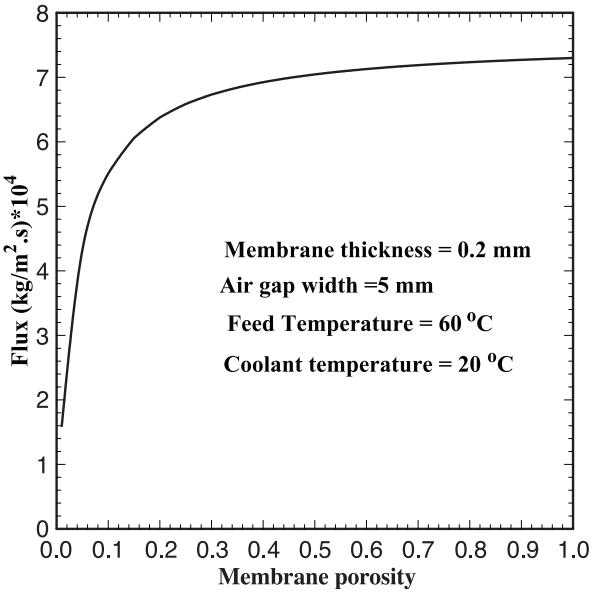

Figure 11. Effect of membrane porosity on mass flux.

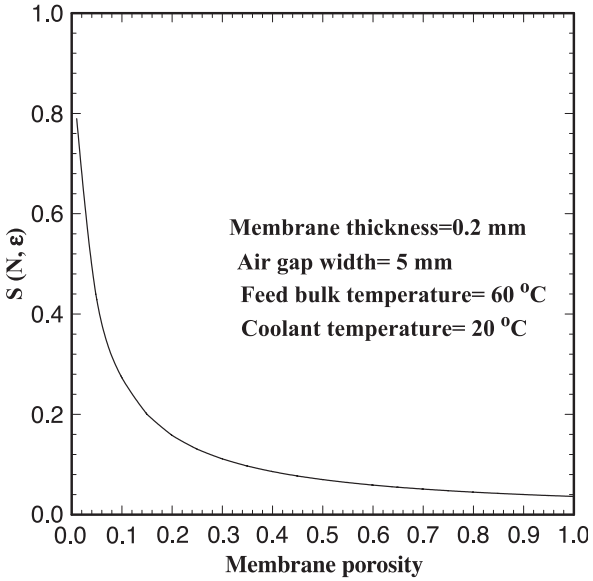

Figure 12. Response of S(N,ε) to membrane porosity.

to any change in membrane porosity. While less sensitivity of mass flux is observed at higher porosity. This result is totally in agreement with that obtained in Figure 11. This can be explained by the fact that at low membrane porosity, the resistance to mass transfer of the membrane is large in comparison with that of the air gap and, thus, an increase in membrane porosity, which decreases its resistance, has a large influence on the flux. At higher membrane porosities, the resistance of the air gap, which is 25 times wider than the membrane, is far more important than that of the membrane and so decreasing the membrane resistance by increasing its porosity has hardly any influence on the flux.

The effect of the membrane porosity on TPF is shown in Figure 13, with the heat transfer coefficients as parameters. The polarization factor decreases slightly by increasing the membrane porosity. When the net pore area available for evaporation is low, the diffusion mass flux is small and, hence, the interfacial temperatures approach each others and the net result is an increase in TPF. However, under given conditions, increasing the heat transfer coefficients increases the mass flux and the heat transfer rate, and this decreases the polarization effect, thus TPF approaches unity. This means that at high values of heat-transfer coefficients, the temperature polarization effect can be neglected.

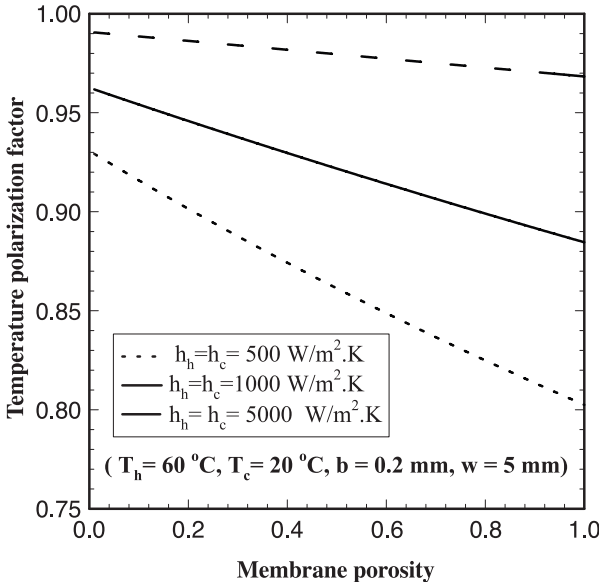

Figure 13. Effect of membrane porosity on temperature polarization factor.

Effect of the Diffusion Path

The length of the diffusion path is an important parameter in determining the mass flux. In Jonsson et al. model, the diffusion path is made up of the membrane thickness, b, and the air gap width, w. As expected, the mass flux decreases when the diffusion path length increases.

The effect of the air gap width on mass flux is shown in Figure 14. The mass flux is inversely proportional to the air gap width. Increasing the air gap increases the diffusion path and this increases the mass transfer resistance and, thus, decreases the flux. The mass flux decreases also by increasing the membrane thickness, as shown in Figure 15, for the same reason.

Figures 16 and 17 show, respectively, the normalized sensitivity of mass flux to the air gap width and membrane thickness. These figures show that both parameters affect the mass flux negetively. Figure 16 shows that at lower air gap width, $-S(N,w) < 0.5$, thus, $-S(N,b) > 0.5$, as shown in Eq. (15). This means that the mass flux is affected negatively by increasing the membrane thickness more than in the air gap width. At higher air gap width, $-S(N,w) \rightarrow 1$, and thus the negative effect of air gap width dominates. However, this conclusion is obtained for small range of w, i.e.,

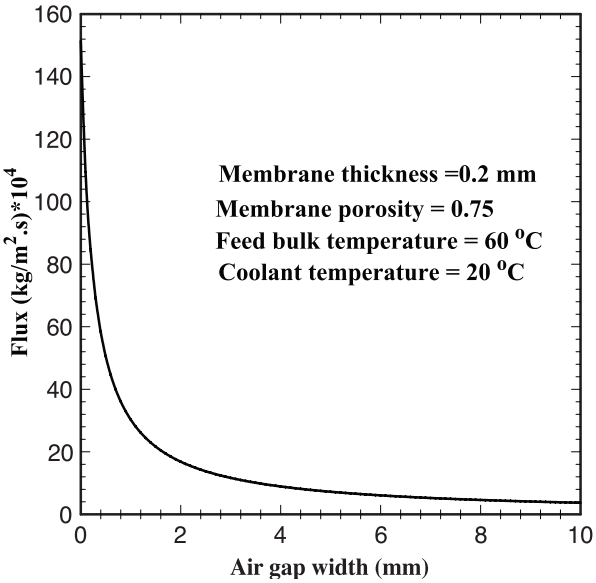

Figure 14. Effect of air gap width on mass flux.

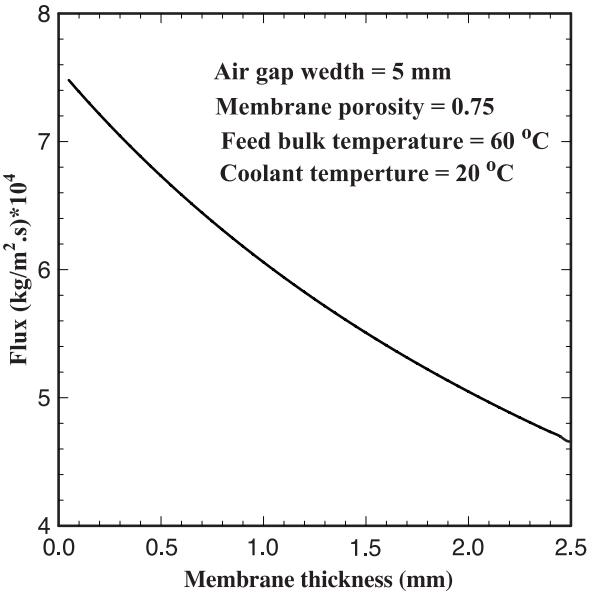

Figure 15. Effect of membrane thickness on mass flux.

Marcel Dekker, Inc.
270 Madison Avenue, New York, New York 10016

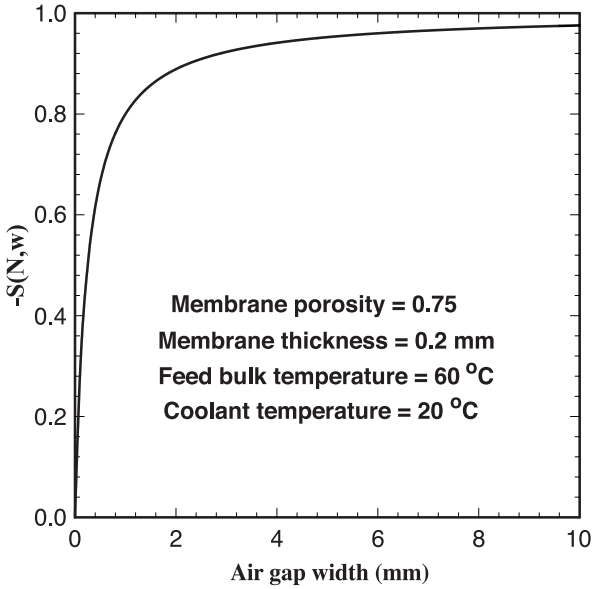

Figure 16. Response of normalized mass flux to air gap width.

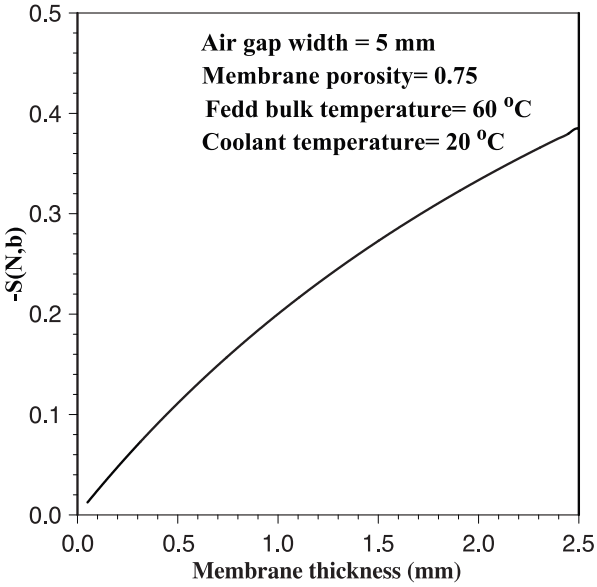

Figure 17. Response of S(N,b) to membrane thickness.

MARCEL DEKKER, INC.
270 Madison Avenue, New York, New York 10016

when the air gap width approaches the membrane thickness. This is supported in Figure 17 in which, for a given air gap width, $-S(N,b)$ is always less than 0.5 and, thus, the negative effect of air gap width on the mass flux dominates.

The total diffusion length, presented in the Banat model, is the sum of air gap width and membrane thickness (i.e., w = air gap + membrane thickness). Figure 18 shows the effect of the length of the diffusion path on the temperature polarization factor with heat-transfer coefficients as parameters. The temperature polarization factor increases significantly with increasing the diffusion path, and this increase is obvious at higher heat transfer coefficients. This is physically attributed to the fact that increasing air gap width makes the interfacial temperatures T_m and T_p closer to T_h and T_c, respectively, and, thus, $(T_m - T_p) \rightarrow (T_h - T_c)$ and, hence, $\theta \rightarrow 1$.

One important conclusion can be obtained from Figure 18, that is, the increase in heat transfer coefficients and the length of the diffusion path lead to a significant effect on the temperature polarization factor. This shows that no direct conclusion can be obtained from the TPF approach about the parametric sensitivity of mass flux. Since at high values of heat-transfer coefficients, the mass flux is high, while at high values of

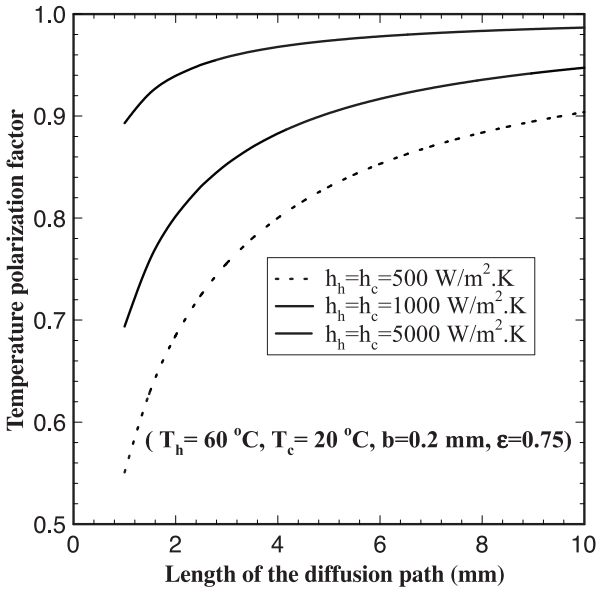

Figure 18. Effect of the diffusion path length on temperature polarization factor.

Marcel Dekker, Inc.
270 Madison Avenue, New York, New York 10016

diffusion path length, the mass flux is low, but in both cases, the TFP approaches unity.

CONCLUSION

The AGMD process was investigated for pure water production. Two models were used: Jonsson et al. model, which is based on approximate solutions in which the temperature polarization effect is neglected; and the Banat and Simandl model, which is based on the Fickian approach where the temperature polarization effect was undertaken. The influence of the relevant parameters on the mass flux was discussed using the Jonsson et al. model and the effect of different parameters on temperature polarization phenomenon was analyzed in detail using the Banat model. It was shown that a satisfactory analysis of the effect and the sensitivity of the various parameters on the mass flux cannot be directly performed using the temperature polarization factor as it was obtained from the normalized sensitivity analysis.

Analysis showed that the mass flux is highly sensitive to the feed bulk temperature in comparison with other parameters, the normalized sensitivity factors of the diffusion path are dependent on each other, and the effect of the air gap width and membrane thickness is inversely proportional to the mass flux. It was found that the assumption of neglecting the temperature polarization effect in the Jonsson et al. model was accepted, under some conditions, to fulfill the needs of sensitivity analysis requirements. Temperature polarization effect may be reduced significantly by increasing the film heat-transfer coefficients. This can be done by increasing the velocities of the liquid streams. The temperature polarization effect can be reduced also by increasing the diffusion path and decreasing the membrane porosity, however, a negligible small flux will be obtained in the later case. Thus, to maximize the water production for commercial membranes, the air gap width must be optimized.

NOMENCLATURE

b	membrane thickness (m)
c	molar concentration (mol/m^3)
D	diffusion coefficient (m^2/s)
h	heat-transfer coefficient ($W/m^2 \cdot K$)
N	mass flux ($kg/m^2 \cdot s$)
P	pressure (N/m^2)

MARCEL DEKKER, INC.
270 Madison Avenue, New York, New York 10016

S normalized sensitivity parameter
T temperature (K)
w air gap width (mm)

Greek Letters

θ temperature polarization factor
λ latent heat of vaporization (J/kg)
ε porosity
τ tortuosity

REFERENCES

1. Abu Al-Rub, F.A.; Banat, F.; Beni-Melhem, K. Parametric sensitivity analysis of direct contact membrane distillation. Sep. Sci. Technol. **2002**, *37*, 3245–3271.
2. Banat, F.A.; Abu Al-Rub, F.A.; Juamah, R.; Shannag, M. Theoretical investigation of membrane distillation role in breaking the formic acid-water azeotropic point: comparison between Fickian and Stefan-Maxwell-based models. Int. Commun. Heat Mass Transfer **1999**, *26*, 879–888.
3. Banat, F.A.; Abu Al-Rub, F.A.; Shannag, M. Simultaneous removal of acetone and ethanol from aqueous solutions by membrane distillation: prediction using the Fick's and the exact and approximate Stefan-Maxwell relations. J. Heat Mass Transfer **1999**, *35*, 423–431.
4. Banat, F.A.; Abu Al-Rub, F.A.; Shannag, M. Modeling of dilute ethanol-water mixture separation by membrane distillation. Sep. Purif. Technol. **1999**, *34*, 119–131.
5. Abu Al-Rub, F.; Banat, F.A.; Shannag, M. Theoretical assessment of dilute acetone removal from aqueous streams by membrane distillation. Sep. Sci. Technol. **1999**, *34*, 2817–2836.
6. Gostoli, C.; Sarti, G.C. Separation of liquid mixtures by membrane distillation. J. Membr. Sci. **1989**, *41*, 211–224.
7. Banat, F.; Simandl, J. Desalination by membrane distillation: a parametric study. Sep. Sci. Technol. **1989**, *33*, 201–226.
8. Jonsson, A.S.; Wimmerstedt, R.; Harrysson, A.C. Membrane distillation, a theoretical study of evaporation through microporous membranes. Desalination **1985**, *56*, 237–250.
9. Andersson, S.I.; Kjellander, N.; Redesjo, B. Design and field tests of a new membrane distillation desalination process. Desalination **1985**, *56*, 345–354.

Marcel Dekker, Inc.
270 Madison Avenue, New York, New York 10016

10. Kimura, S.; Nakao, S. Transport phenomena in membrane distillation. J. Membr. Sci. **1987**, *33*, 285–298.
11. Kubota, S.; Ohta, K.; Hayaro, I.; Hirai, M.; Kikuchi, K.; Murayama, M. Experiments on seawater desalination by membrane distillation. Desalination **1988**, *69*, 19–26.
12. Ohta, K.; Kikuchi, K.; Hayano, I.; Okabe, T.; Goto, T.; Kimura, S. Experiments on sea water desalination by membrane distillation. Desalination **1990**, *78*, 177–185.
13. Ohta, K.; Hayano, I.; Okaba, T.; Kimura, S.; Ohya, H. Membrane distillation with fluro-carbon membranes. Desalination **1991**, *81*, 107–115.
14. Udriot, H.; Araque, A.; Stockar, U. Azotropic mixtures may be broken by membrane distillation. Chem. Eng. J. **1994**, *54*, 87–93.
15. Banat, F.A.; Abu Al-Rub, F.A.; Juamah, R.; Shannag, M. On the effect of inert gases in breaking the formic acid-water on azeotrope by gas gap membrane distillation. J. Chem. Eng. **1999**, *73*, 37–42.
16. Liu, G.L.; Zhu, C.; Cheung, C.S.; Leung, C.W. Theoretical and experimental studies on air gap membrane distillation. Heat Mass Transfer **1998**, *43*, 329–335.
17. Zhu, C.; Liu, G.L.; Cheung, C.S.; Leung, C.W.; Zhu, Z.C. Ultrasonic stimulation on enhancement of air gap membrane distillation. J. Membr. Sci. **1999**, *161*, 85–93.
18. Kurokawa, H.; Kuroda, O.; Takasashi, S.; Ebara, K. Vapor permeate characteristics of membrane distillation. Sep. Sci. Technol. **1990**, *25*, 1349–1359.
19. Sherwood, T.K.; Pigford, R.L.; Wilke, C.R. *Mass Transfer*; McGraw Hill, 1975.
20. Bandini, S.; Gostoli, C.; Sarti, G.C. Role of heat and mass transfer in membrane distillation process. Desalination **1991**, *81*, 91–106.
21. Miguel, A.; Jose, M.; Fernanda, S.; Rosa, N.; Julia, S. Application of parameteric sensitivity to batch process safety: theoretical and experimental studies. Chem. Eng. Technol. **1996**, *19*, 222–232.

Received October 2002
Revised April 2003

MARCEL DEKKER, INC.
270 Madison Avenue, New York, New York 10016